Linearized electro-optic modulators based on a two-section Y-fed directional coupler

Beomsuk Lee,[1,*] Che-Yun Lin,[1] Alan X. Wang,[2] Raluca Dinu,[3] and Ray T. Chen[1]

[1]The University of Texas at Austin, 10100 Burnet Road, Austin, Texas 78758, USA

[2]Omega Optics, Inc., 10306 Sausalito Drive, Austin, Texas 78759, USA

[3]GigOptix, Inc., 19910 North Creek Parkway, Suite 100, Bothell, Washington 98011, USA

*Corresponding author: bslee74@gmail.com

Received 16 September 2010; accepted 11 October 2010;
posted 19 October 2010 (Doc. ID 135239); published 17 November 2010

We experimentally demonstrate a linearized Y-fed directional coupler (DC) modulator based on an electro-optic (EO) polymer waveguide. The spurious free dynamic range of 119 dB/Hz$^{2/3}$, which is 11 dB higher than that of the conventional Mach–Zehnder modulator, is achieved by introducing the reversed $\Delta\beta$ technique in the two-section Y-fed DC. The in-device EO coefficient (r_{33}) of the fabricated device is as high as 79 pm/V in 1.55 μm wavelength, which is 88% of a single film r_{33} of LPD-80/APC

OCIS codes: 060.4080, 060.4510, 250.2080, 250.4110, 250.5460, 250.7360.

1. Introduction

The dynamic range of analog optical links is limited by the linearity of the system components such as amplifiers, detectors, and modulators. Various linearization schemes have been proposed to improve the linearity of the modulators. These include dual polarization [1], dual parallel [2], and electronic compensation [3,4] schemes in Mach–Zehnder (MZ) modulators. However, these schemes require multiple modulators or complicated modulation synchronization, which hinders their practical implementation. Directional coupler (DC) modulators, on the other hand, can provide high linearity without such complicated structures or circuits. Even higher linearity can be achieved by introducing the reversed $\Delta\beta$ technique [5–9], where $\Delta\beta$ is the propagation constant mismatch between the two coupled waveguides. In this paper, we demonstrate a linearized DC modulator based on an electro-optic (EO) polymer. The spurious free dynamic range (SFDR) of 119 dB/Hz$^{2/3}$, which is 11 dB higher than that of the conventional MZ modulator, is achieved by employing the reversed $\Delta\beta$ technique in the two-section Y-fed directional coupler (YFDC) modulator. Also, a high in-device EO coefficient (r_{33}) of 79 pm/V is achieved by using LPD-80/amorphous polycarbonate (APC).

2. Principle of Operation

A schematic of the YFDC is shown in Fig. 1. Unlike the conventional DC, one input waveguide branches into a pair of symmetric waveguides that are optically coupled with each other. Because of the symmetry, equal optical power with the same phase is launched into the coupled waveguides and, hence, the operating point is automatically set at the 3 dB point without bias voltage. $\Delta\beta$ reversal can be realized by applying voltages with opposite polarity to the two sections of electrode, as illustrated in Fig. 1(a), which is the original proposal in [5]. The advantage of this configuration is that voltages applied to each section can be controlled independently, and, hence, the variation of the coupling coefficient caused by fabrication imperfections can be compensated for by simple electrical adjustment. However, the requirement for multiple rf sources makes this configuration incompatible with high-speed analog optical links. Alternatively,

0003-6935/10/336485-04$15.00/0

equivalent $\Delta\beta$ reversal can be realized by domain-inversion poling of EO polymer, as shown in Fig. 1(b). When EO polymer dipoles are poled in the opposite direction in the two sections of DC, $\Delta\beta$ reversal is induced by a single uniform traveling wave electrode [10]. The configuration in Fig. 1(c) is based on a lumped element electrode that alternately zigzags from one waveguide to the other. This configuration creates equivalent $\Delta\beta$ reversal without domain-inversion poling of EO polymer (pseudo domain inversion) but is limited to low-speed operation. The configuration in Fig. 1(c) is adopted in this demonstration as a proof of concept to investigate the linearity enhancement by $\Delta\beta$ reversal. The configuration in Fig. 1(b) is currently under way for demonstration of high-speed linearized modulators.

3. Design and Fabrication

Suppression of the nonlinear distortions, specifically the third-order intermodulation distortions (IMD3s) in the scope of this paper, in the two-section YFDC modulator can be calculated as a function of the normalized interaction lengths (S_1 and S_2 in Fig. 1) of the two sections. Relative IMD3 suppression can be graphically compared by plotting the calculated IMD3 suppressions on the (S_1, S_2) plane. The procedure and results can be found in [7]. $S_1 = S_2 = 2.85$ is chosen for the test in this paper because it provides excellent linearity as well as a very large modulation depth.

An exploded schematic of the two-section YFDC modulator with pseudo domain inversion is shown in Fig. 2(a). The physical parameters of the DC waveguides are calculated by R-Soft (BeamPROP). Given the refractive index and thickness of the cladding polymers (UV-15LV, 1.50 and 2.5 μm; UFC-170A, 1.49 and 2 μm) and the core EO polymer (LPD-80/APC, 1.70 and 2.2 μm), a pair of single-mode waveguides with 5 μm width and 0.52 μm trench separated by a 5 μm gap forms a DC as indicated in Fig. 2(a) with the coupling length of 3550 μm (not shown) at a 1.55 μm wavelength. The resulting total interaction length is about 2 cm.

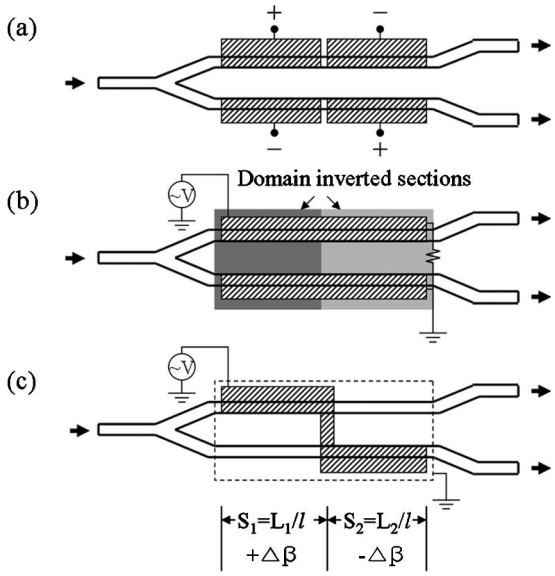

Fig. 1. Schematic of YFDC modulators with (a) two-section electrode with reversed $\Delta\beta$, (b) single uniform traveling wave electrode with two-section domain inversion, and (c) single lumped element electrode with two-section pseudo domain inversion (S, normalized interaction length of each section; L, interaction length of each section; and l, coupling length of the DC).

Devices are fabricated by standard polymer processes including spin coating, UV curing, photolithography, and oxygen plasma reactive ion etching (RIE). The bottom cladding layer (UV-15LV) is spin coated on top of the ground electrode (aluminum). Waveguides are defined on the bottom cladding layer by photolithography and oxygen plasma RIE. The core EO polymer (LPD-80/APC with 50 wt.% loading) and the top cladding layer (UFC-170A) are spin coated on the patterned waveguides. Both UFC-170A and UV-15LV are cured by UV light under nitrogen purging. The cross-sectional scanning electron micrograph of the fabricated waveguides is shown in Fig. 2(b). The core EO polymer is usually poled after the top cladding layer is spin coated. In this fabrication, the sequence is reversed, i.e., LPD-80/APC is poled by the contact poling technique (poling field, 100 V/μm; peak temperature, 130 °C) before the top cladding layer is spin coated. It has been known that the high resistivity of the cladding polymers screens a significant part of the poling electric field seen by the core EO polymer and thus lowers the poling efficiency [11]. The decrease in poling efficiency often results in an in-device r_{33} that is ~30% of a standalone film [12]. Following the reversed sequence, the voltage drop across the top cladding polymer can be avoided and thus the increased poling electric field across the core EO polymer improves the poling efficiency. The driving electrode (gold) is patterned on the top cladding layer by photolithography and wet etching with precise alignment with waveguides. Finally, the fabricated devices are cleaved and polished for testing.

4. Measurement and Results

Fabricated devices are tested on a six-axis auto-aligner system. Transverse magnetic (TM) field

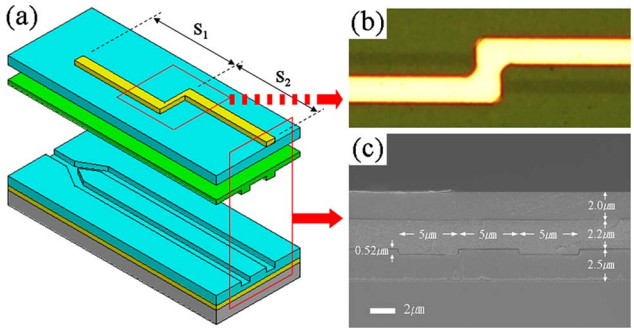

Fig. 2. (Color online) (a) Exploded schematic of the two-section YFDC modulator with pseudo domain inversion ($S_1 = S_2 = 2.85$), (b) top view of the driving electrode aligned with waveguides, and (c) cross-sectional scanning electron micrograph of the fabricated waveguides.

polarized light from a tunable laser is launched into the input waveguide by a polarization maintaining fiber. The modulated optical signals are collected by a single-mode fiber and converted to electrical signals by a photodetector with a built-in amplifier. With 10 mW of input optical power, the output optical power from one of the DC waveguides is measured to be 40 μW, which translates into the total insertion loss of ~21 dB.

The transfer function of the linearized two-section YFDC modulator is shown in Fig. 3. The device is overmodulated by 10 V_{pp} at 1 kHz in the 1.55 μm wavelength, and the measured switching voltage is 6.1 V. The switching condition can be written in general as $|\Delta\beta \cdot L| = p\pi$ [13], where $\Delta\beta$ is $\frac{2\pi}{\lambda}\Delta n = \frac{\pi n^3 r_{33}\Gamma V}{\lambda d}$ (n, effective index; r_{33}, EO coefficient; Γ, overlap integral between optical mode and electric field; V, switching voltage; λ, operation wavelength; and d, electrode separation), L is the total interaction length, and p is a parameter dependent on the modulator type. For the two-section YFDC with $S_1 = S_2 = 2.85$, p is calculated to be 4.19 in [7]. Given $n = 1.68$, $\Gamma = 0.85$, $\lambda = 1.55$ μm, and $d = 6.7$ μm, the in-device r_{33} is 79 pm/V, which is 88% of the single film r_{33} [14]. This in-device poling efficiency is higher than that in our previous report [15], where EO polymer (AJLS102/APC) was poled after the top cladding layer was spin coated, resulting in 56% of the single film r_{33}.

A two-tone test is performed to analyze the linearity of the fabricated devices in the 1.55 μm wavelength. Two input signals ($f_1 = 19$ and $f_2 = 21$ kHz) generated by a multifunction synthesizer are mixed and applied to the devices, and the resulting output fundamentals and IMD3s ($f_1 \times 2 - f_2 = 17$ and $f_2 \times 2 - f_1 = 23$ kHz) are analyzed by a microwave spectrum analyzer. Measured fundamentals and IMD3s are plotted as a function of input powers, as shown in Fig. 4. An important figure of merit in analog optical links is the SFDR, which is the ratio of the largest to smallest signal that can be transmitted and received in the links without introducing unacceptable distortions [8]. The SFDR can be graphically determined, as illustrated in Fig. 4. Measured IMD3s are extrapolated to find the intercept point with the noise floor. The difference between the fundamental

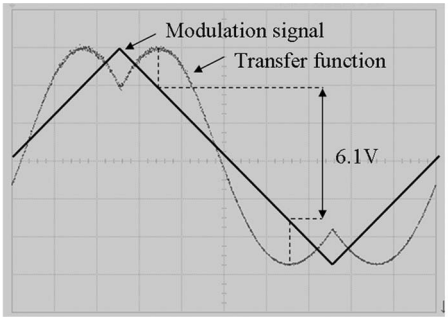

Fig. 3. Transfer function of the linearized two-section YFDC modulator. (The input optical wavelength is 1.55 μm. The device is overmodulated by 10 V_{pp} at 1 kHz.)

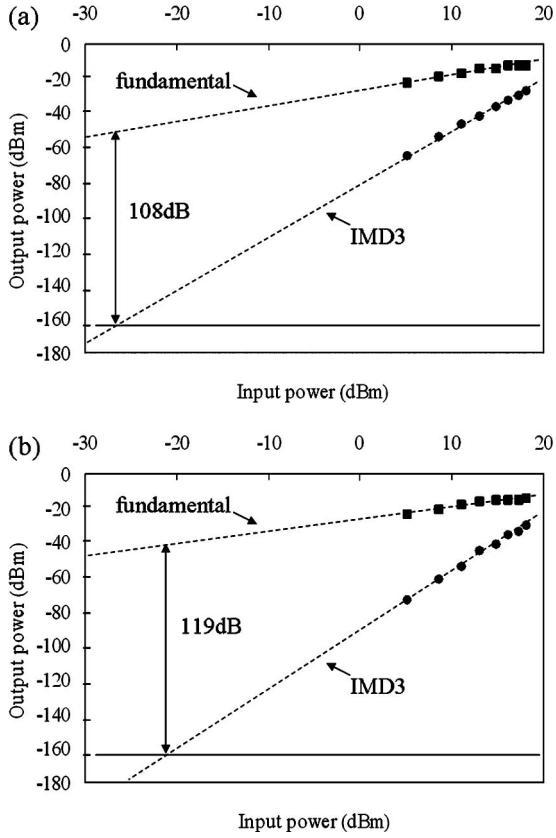

Fig. 4. Two-tone test results of (a) a conventional MZ modulator and (b) a linearized two-section YFDC modulator. (Input optical wavelength is 1.55 μm. Fundamental frequencies are 19 and 21 kHz, and the resulting IMD3 frequencies are 17 and 23 kHz. Squares are measured output power of the fundamental signals and dots are that of the IMD3 signals. Dashed lines are the extrapolation of measured data points.)

and IMD3 at the intercepted input power is the SFDR of the analyzed device. Considering the relative intensity noise of the distributed feedback laser and the shot noise of the photodiode, it is very difficult to achieve a noise floor below −145 dBm in real analog optical links [7]. However, laboratory test results are often presented assuming the noise floor at −160 dBm [16]. With the noise floor at −160 dBm, the SFDR of the linearized YFDC modulator is 119 $dB/Hz^{2/3}$ in Fig. 4(b), which is 11 dB higher than that of the conventional MZ modulator in Fig. 4(a). It should be noted that the measurement includes distortions from the amplifier as well as from the device.

5. Conclusion

A linearized EO polymer modulator is realized by introducing the reversed $\Delta\beta$ technique in the two-section YFDC. The SFDR of 119 $dB/Hz^{2/3}$ is achieved with an 11 dB enhancement over the conventional MZ modulator. The in-device r_{33} of the EO polymer is also improved by simply modifying the fabrication procedure.

This work was supported by the Defense Advanced Research Projects Agency (DARPA) under contract W31P4Q-08-C-0160, monitored by Devnand Shenoy.

References

1. L. M. Johnson and H. V. Roussell, "Reduction of intermodulation distortion in interferometric optical modulators," Opt. Lett. **13**, 928–930 (1988).
2. S. K. Korotky and R. M. de Ridder, "Dual parallel modulation schemes for low-distortion analog optical transmission," IEEE J. Select. Areas Commun. **8**, 1377–1381 (1990).
3. R. B. Childs and V. A. O'Bryne, "Predistortion linearization of directly modulated DFB lasers and external modulators for AM video transmission," in *Optical Fiber Communication*, OSA Technical Digest (Optical Society of America, 1990), paper WH6.
4. Y. Chiu, B. Jalali, S. Garner, and W. Steier, "Broad-band electronic linearizer for externally modulated analog fiber-optic links," IEEE Photon. Technol. Lett. **11**, 48–50 (1999).
5. H. Kogelnik and R. Schmidt, "Switched directional couplers with alternating $\Delta\beta$," IEEE J. Quantum Electron. **12**, 396–401 (1976).
6. R. F. Tavlykaev and R. V. Ramaswamy, "Highly linear Y-fed directional coupler modulator with low intermodulation distortion," J. Lightwave Technol. **17**, 282–291 (1999).
7. X. Wang, B.-S. Lee, C.-Y. Lin, D. An, and R. T. Chen, "Electro-optic polymer linear modulators based on multiple-domain Y-fed directional coupler," J. Lightwave Technol. **28**, 1670–1676 (2010).
8. J. H. Schaffner, J. F. Lam, C. J. Gaeta, G. L. Tangonan, R. L. Joyce, M. L. Farwell, and W. S. C. Chang, "Spur-free dynamic range measurements of a fiber optic link with traveling wave linearized directional coupler modulators," IEEE Photon. Technol. Lett. **6**, 273–275 (1994).
9. T. Kishino, R. F. Tavlykaev, and R. V. Ramaswamy, "A Y-fed directional coupler modulator with a highly linear transfer curve," IEEE Photon. Technol. Lett. **12**, 1474–1476 (2000).
10. D. An, S. Tang, Z. Yue, J. Taboada, L. Sun, Z. Han, X. Lu, and R. T. Chen, "Linearized Y-coupler modulator based on domain-inverted polymeric waveguide," Proc. SPIE **3632**, 220–231 (1999).
11. P. R. Ashley, E. A. Sornsin, U. Command, and R. Arsenal, "Doped optical claddings for waveguide devices with electrooptical polymers," IEEE Photon. Technol. Lett. **4**, 1026–1028 (1992).
12. Y. H. Kuo, L. Jingdong, W. H. Steier, and A. K. Y. Jen, "Enhanced thermal stability of electrooptic polymer modulators using the Diels-Alder crosslinkable polymer," IEEE Photon. Technol. Lett. **18**, 175–177 (2006).
13. R. C. Alferness, "Waveguide electrooptic modulators," IEEE Trans. Microwave Theory Tech. **30**, 1121–1137 (1982).
14. H. Chen, B. Chen, D. Huang, D. Jin, J. D. Luo, A. K.-Y. Jen, and R. Dinu, "Broadband electro-optic polymer modulators with high electro-optic activity and low poling induced optical loss," Appl. Phys. Lett. **93**, 043507 (2008).
15. B. Lee, C. Lin, X. Wang, R. T. Chen, J. Luo, and A. K.-Y. Jen, "Bias-free electro-optic polymer-based two-section Y-branch waveguide modulator with 22 dB linearity enhancement," Opt. Lett. **34**, 3277–3279 (2009).
16. Y.-C. Hung, S. K. Kim, and H. Fetterman, "Experimental demonstration of a linearized polymeric directional coupler modulator," IEEE Photon. Technol. Lett. **19**, 1762–1764 (2007).